Comparative Evaluation of Color Characterization and Gamut of LCDs versus CRTs

Gaurav Sharma

Xerox Corp., MS0128-27E, 800 Phillips Rd., Webster, NY 14580

ABSTRACT

Liquid-crystal-displays (LCDs) and cathode-ray-tubes (CRTs) are compared with regard to color-calibration and color gamut. Applicability of common display calibration models to LCDs and CRTs is experimentally tested. Color-calibration accuracy, ease of calibration, and achievable color gamut are evaluated for the displays. An offset, matrix, and tone-response correction model is found to be suitable for color calibration of LCDs for most applications. The model, however, results in larger calibration error for LCDs than for CRTs, and unlike CRTs a power law tone-response correction is unsuitable for LCDs. A very significant color variation is seen with change in viewing angle for the prototype LCD display employed in the study. The LCD display provides a significantly larger color gamut under typical viewing conditions than CRTs, primarily due to higher luminance.

Keywords: liquid-crystal-displays, LCD, CRT, display color gamut, CRT gamut, color calibration.

1. INTRODUCTION

As a result of significant cost and quality improvements Liquid Crystal displays (LCDs) are poised to replace cathode-ray-tubes (CRTs) as the primary computer displays.[1,2] While LCDs originally found a niche in portable computers on account of their compact size and low power consumption, they are now available at increasingly higher spatial-resolutions and in larger screen sizes with image quality that meets or exceeds that of typical cathode-ray-tube (CRT) displays.[3]

With the widespread use of LCDs, there is also an increased need for color management for these displays. While the color characteristics of CRT displays and methods for their color calibration have been extensively studied and reported,[4–9] the color characteristics of LCD displays and methods for calibration have only come to the fore-front in the last few years and have received only limited attention in published literature.[10–13]

Active-matrix LCDs (AMLCDs) represent the most commonly employed LCD display technology for computer displays. This paper reviews the color characteristics and the color-calibration requirements for AMLCDs and contrasts them with CRT displays which represent the pre-dominant display technology employed today.

2. DISPLAY COLOR-CALIBRATION MODELS

Abstraction of the display characteristics in the form of a mathematical model is useful for the discussion of color calibration. Under suitable simplifying assumptions,[13] the operation of the display may be modeled mathematically as a radiance spectrum,

$$f(\lambda; R, G, B) \quad , \tag{1}$$

for each triplet of R, G, B driving values, where λ denotes the wavelength. For color measurement and control, the visible region of the electromagnetic spectrum covering a wavelength range roughly from $\lambda_{min} = 400$nm to $\lambda_{max} = 700$nm is of interest. The color corresponding to the radiance spectrum can then be measured and specified using the CIE system,[14] wherein color corresponding to the radiance spectrum is specified by a "tristimulus" vector $\mathbf{t}(R, G, B) = [t_1, t_2, t_3]^T$ of the XYZ tristimulus coordinates * given by

$$t_i = \int_{\lambda_{min}}^{\lambda_{max}} c_i(\lambda) f(\lambda; R, G, B) \, d\lambda \tag{2}$$

Further author information: Email: g.sharma@ieee.org, Web: http://chester.xerox.com/~sharma

*For a tutorial survey of color imaging that introduces terminology and notation consistent with the current paper, the reader is referred to Sharma *et al.*[15,16]

where t_1, t_2, t_3 are respectively, the CIE X, Y, and Z tristimulus values and $c_1(\lambda), c_2(\lambda), c_3(\lambda)$ are respectively, the CIE 2-degree color matching functions[14] $\bar{x}(\lambda)$, $\bar{y}(\lambda)$, $\bar{z}(\lambda)$.

The generic mathematical model of a display as a radiance distribution for each driving RGB triplet value is complex and requires a large number of measurements for color characterization. The design and operating physics of displays often ensures that the red, green, and blue channels function independently of each other and this assumption of channel-independence is commonly employed in color characterization models. Mathematically, the channel-independence assumption implies that the radiance spectrum corresponding to an RGB value can be separated into functions dependent only on the R, G and B values, i.e.,

$$f(\lambda; R, G, B) = f_r(\lambda, R) + f_g(\lambda, G) + f_b(\lambda, B) + f_0(\lambda) \tag{3}$$

where $f_r(\lambda, R)$ represents the light produced by the red channel in response to the input value R, and in a similar fashion $f_g(\lambda, G)$ and $f_b(\lambda, B)$ represent the light from the green and blue channels, respectively, and $f_0(\lambda)$ accounts for light reflected by the display (flare) and/or light emitted from a pixel with R=0, G=0, B=0.

The channel-independence assumption allows the complete characterization of the display based on a characterization of the individual RGB channels. It therefore reduces the problem of color characterization of the display from a three-dimensional characterization into three much simpler one-dimensional characterizations. The problem can be simplified further using the additional assumption that

$$f_r(\lambda, R) = v_r(R)s_r(\lambda) \tag{4}$$

where $s_r(\lambda)$ represents the radiance spectra of the light from the red channel at the maximum value of the red driving signal, and $v_r(R)$ denotes the amplitude scaling factor. Note that by virtue of our definition $0 \leq v_r(R) \leq 1$. For the green and blue channels, the assumption results in similar decompositions: $f_g(\lambda, G) = v_g(G)s_g(\lambda)$ and $f_b(\lambda, B) = v_b(B)s_b(\lambda)$, where the terms are defined analogously to those for the red channel. The functions $v_r()$, $v_g()$, and $v_b()$ are commonly referred to as the tone-response-curves (TRCs) of the red, green, and blue channels and are typically monotonic functions over the range 0 to 1.

From the linearity of (2), it follows that the assumptions of (3) and (4) can alternately be written in terms of the tristimulus values instead of spectra, as

$$\mathbf{t}(R, G, B) = \mathbf{t}_r(R) + \mathbf{t}_g(G) + \mathbf{t}_b(B) + \mathbf{t}_0 \tag{5}$$

$$\mathbf{t}_r(R) = v_r(R)\mathbf{t}_{mr}; \quad \mathbf{t}_g(G) = v_g(G)\mathbf{t}_{mg}; \quad \mathbf{t}_b(B) = v_b(B)\mathbf{t}_{mb} \tag{6}$$

where the bold face tristimulus terms in (5) represent the tristimulus values corresponding to the spectral terms defined earlier, $\mathbf{t}_{mr}$, $\mathbf{t}_{mg}$, and $\mathbf{t}_{mb}$ represent the tristimulus values at the maximum driving signal for the red, green and blue channels, respectively. The complete model of (5)–(6) is shown graphically in Fig. 1. Eqns. (5)–(6), can be combined as

$$\begin{aligned} \mathbf{t}(R, G, B) &= [\mathbf{t}_{mr}, \mathbf{t}_{mg}, \mathbf{t}_{mb}][v_r(R), v_g(G), v_b(B)]^T + \mathbf{t}_0 \tag{7}\\ &= \mathbf{T}_m[v_r(R), v_g(G), v_b(B)]^T + \mathbf{t}_0 \tag{8} \end{aligned}$$

where $\mathbf{T}_m \equiv [\mathbf{t}_{mr}, \mathbf{t}_{mg}, \mathbf{t}_{mb}]$ is the matrix with the maximum amplitude tristimuli for the RGB channels as its columns. Note that equations (6) imply that the CIE x, y chromaticity coordinates[14, 15, 17] of a channel remain constant independent of the value of the driving signal for that channel. This is referred to as the "channel-chromaticity-constancy assumption".

Practical use of the display color calibration requires the inverse of the device characterization model, which provides the R, G, B values corresponding to a desired tristimulus value. The model of (8) can be readily inverted to obtain the R, G, B values corresponding to an (achievable) desired tristimulus value $\mathbf{t}$ as

$$\begin{aligned} [R, G, B] &= \left[v_r^{-1}(R'), v_g^{-1}(G'), v_b^{-1}(B')\right] \tag{9}\\ [R', G', B'] &= \mathbf{T}_m^{-1}(\mathbf{t} - \mathbf{t}_0) \tag{10} \end{aligned}$$
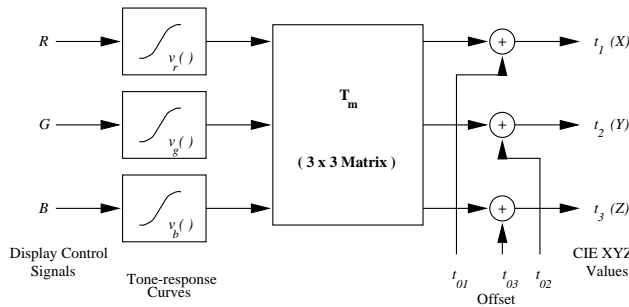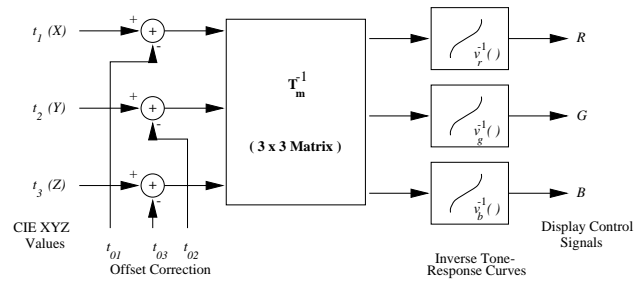
Figure 1: Display forward-model.

Figure 2: Display inverse-model.

From the above discussion, it is apparent that for the simplified model of (5)–(6), the inverse-model is readily computed using the inverse of the 1-dimensional TRCs for each of the channels and the inverse of the 3×3 matrix $\mathbf{T}_m$. This is significantly simpler than direct numerical computation of the 3-dimensional forward-model for the display represented. The matrix-inverse and the inverse of the TRCs may be pre-computed, and the latter may be computationally implemented as a 1-D look-up-table (LUT). Fig. 2 graphically illustrates this inverse-model, depicting the process of converting from CIEXYZ to display RGB using an offset-correction, 3x3 matrix, and inverse tone-response corrections. In order to display a calibrated image on the display, these operations would need to be applied to each pixel as the color-correction step. The inverse-model of (9)–(10) is fairly computationally-efficient and can be directly used for mapping of images into display RGB color-coordinates prior to display. As opposed to this, the more general models of (1) and (3) require intensive computation for the determination of the inverse. The run-time mapping of images to display coordinates for these general models relies on memory intensive 3-dimensional LUTs that store the inverse-model.

3. CRT COLOR CALIBRATION

The models of Section 2 have been successfully applied to the characterization of CRT monitors since the early 1980's.[4] The physics of CRTs strongly supports the assumptions of channel-independence and channel-chromaticity-constancy and they have also been extensively validated in experiments.[5,9] For CRTs the final model of Section 2, can be further simplified by using a parametric mathematical model for the TRCs for the individual channels that is derived from the power-law relation between grid-voltage and beam-current for a vacuum tube.[18,19] The expression for the red channel TRC resulting from the power-law relation can be written as[8,20]

$$v_r(R) = \left((1 - \beta_r) \frac{R}{R_{max}} + \beta_r \right)^{\gamma_r} \tag{11}$$

where R_{max} corresponds to the maximum value for the red-channel signal, and β_r and γ_r represent the offset and exponent parameters of the model. Analogous expressions apply for the green and blue channels. For appropriate set-up of the monitor offset and brightness controls,[8] the offset term $\beta_r = 0$ and the relation simplifies to a power-law relation, which has been commonly-used power-law for CRTs.[21] The exponents for the three channels are typically equal and their value is commonly referred to as the "gamma" of the CRT. The numerical value of gamma for a CRT is typically around 2.2 though the effective "gamma" seen by an application may be influenced by the display and operating system settings.[22] With the power-law parametric form for the TRCs, the inverse model of eqn. (9) reduces to another power law correction, which is commonly referred to as gamma-correction. Most present day CRT monitors are manufactured using the same set of red, green, and blue phosphors and the power-law relation is a fundamental characteristic of vacuum tubes. CRTs therefore tend to be fairly close to each other in their basic color characteristics.

4. AMLCD DISPLAY COLOR CALIBRATION

The most common LCD displays for computers are back-lit active-matrix LCDs (AMLCDs) of the "twisted nematic" type.[23] The physics of operation of typical AMLCDs provides reasonable support for the assumptions of

channel independence and channel chromaticity constancy.[13] The model of (8) is therefore a suitable candidate for characterization of AMLCDs. The parametric power-law relation of (11) is however poorly matched to the typical TRCs of AMLCDs.

A prototype LCD display[24] was chosen for experimental study in order to evaluate the applicability of the color-calibration models of Section 2 to LCDs. A commercially available CRT monitor was also studied in parallel to provide comparative data. For the purposes of color characterization and evaluation, on either display, a number of spatially uniform color patches were displayed in the central region and measured using a PR705 spectroradiometer that provides full spectral radiance for each of the patches at a 2nm sampling resolution in the range 380 to 780nm. The patches were partitioned *a priori* into a characterization-set used for performing the color calibration and an independent test-set for evaluating the accuracy of the characterization. All measurements were made at a 0-degree viewing-angle (with respect to the normal to the screen). The measurements for the patches were made in a dark room with minimal stray light. Flare (reflection from the display screen) for normal viewing conditions was measured independently for each of the displays with typical room lighting turned on.

The characterization patches consisted of ramps with 33 levels each for each of the R, G, B channels (e.g., the red-channel characterization patches consisted of patches with $G = B = 0$, and R values uniformly sampling the range from 0 to $R_{max} = 255$). The test-set consisted of 64 independent test patches representing a $4 \times 4 \times 4$ uniform sampling of the RGB cube.

The TRCs $v_r()$, $v_g()$, and $v_b()$ for the red, green and blue channels were estimated from the spectral measurements of the characterization patches using a least-squares procedure.[13] These are shown in Fig. 3. Note that the TRCs have the characteristic S-shape expected from the raw opto-electronic responses for an LCD pixel. Also note that the TRCs for red, green and blue channels are not identical.

For the purposes of comparison, the data measured from CRT was analyzed using identical procedures. The CRT TRCs for the red, green, and blue channels are shown in Fig. 4. The TRCs are in agreement with the power-law (gamma) relationship of (11) (the best approximations for the gamma for the red, green, and blue channels were 2.34, 2.36, and 2.43, respectively.). Compared to the LCD display TRCs, the TRCs for the CRT RGB channels are fairly close to each other.

With the assumptions of channel-independence and channel-chromaticity constancy, the per-channel spectral characterizations can be used with the model of (3)-(4) to predict the spectral radiance for the display corresponding to any RGB value. For both the LCD and the CRT display, predictions for the 64 independent test patches (representing a 4x4x4 uniform sampling of the RGB cube) were made using the TRCs determined earlier. These predictions were compared with the actual measurements for the test patches and color errors
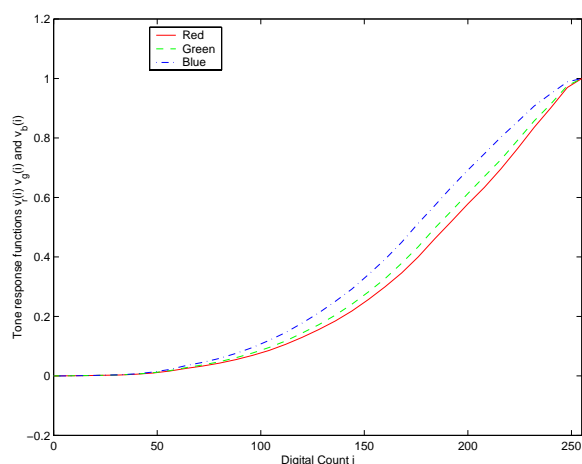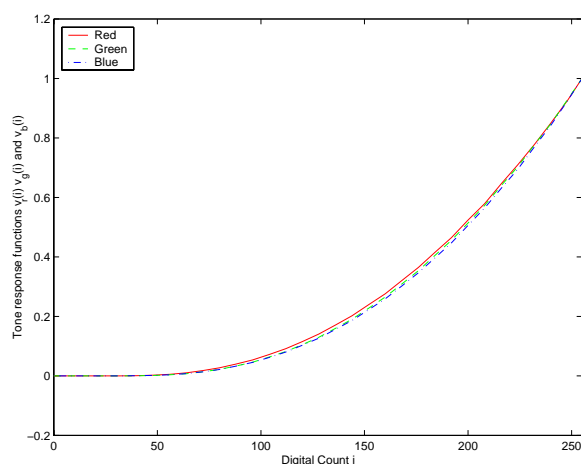

Figure 3: LCD R,G,B channel TRCs.

Figure 4: CRT R, G, B, channel TRCs.

Table 1: LCD & CRT Display Color-Calibration Errors.

Sample Set		Color-Calibration Errors			
		$\triangle E_{ab}^*$ units		$\triangle E_{94}^*$ units	
		Mean	Max.	Mean	Max
LCD	Characterization RGB ramps	2.01	6.94	0.87	2.76
	Test $4 \times 4 \times 4$ RGB cube	2.32	4.49	1.09	2.07
CRT	Characterization RGB ramps	0.18	1.11	0.09	0.42
	Test $4 \times 4 \times 4$ RGB cube	0.40	0.89	0.23	0.68

Table 2: Color-Calibration Errors for LCD and CRT displays over test samples with a "gamma-offset" TRC model.

Error over Test Set ($4 \times 4 \times 4$ RGB cube)	Color-Calibration Errors			
	$\triangle E_{ab}^*$ units		$\triangle E_{94}^*$ units	
	Mean	Max.	Mean	Max
LCD display	4.95	12.30	2.44	7.66
CRT display	0.71	1.84	0.42	1.60

were computed in $\triangle E_{ab}^*$[14] and $\triangle E_{94}^*$[25] units. These errors are tabulated in Table 1 for the LCD and CRT displays. The table reports the errors over the characterization RGB ramps and the test patches separately, and both the average and maximum color errors over each of these data sets are tabulated.

For the CRT display, the color errors from the calibration model are extremely small, with even the maximum color error under 1.0 $\triangle E_{94}^*$ unit. This indicates that Eqns. (5)-(6) model the operation of the CRT remarkably well. For the LCD display, the average color error over the test set is just around 1.0 $\triangle E_{94}^*$ unit and the maximum errors is around 2.0 $\triangle E_{94}^*$. This level of error is acceptable for most imaging applications and therefore the forward-model of Fig. 1 and the inverse-model of Fig. 2 can be applied for the color calibration of LCD displays, for all but the most critical imaging applications.

Since several commercial image processing packages allow for easy "gamma-correction" of images, it is also worth determining how closely the the power-law based model of (11) represents the display TRCs. For both the LCD display and the CRT, the best "gamma" exponent and offset values for each of the channels were determined through a least-squares fit of the TRCs to (11). The power-law TRCs corresponding to the estimated gamma and offset values from (11) were then used in the forward-model of (5)-(6) to obtain predicted tristimulus values for the test samples, and color errors were computed as before. The resulting mean and maximum color errors in $\triangle E_{ab}^*$ and $\triangle E_{94}^*$ units for the LCD and the CRT display are reported in Table 2. Note that the calibration errors for the CRT are only moderately higher than the corresponding ones in Table 1, however, the errors for the LCD display are much larger than those in Table 1. Thus the parametric model of (11) is clearly unsuitable for representing the TRCs of LCD displays and color-calibration techniques that rely on the parametric model for display calibration[26–28] should not be employed for LCD displays.

In addition to the results presented herein the LCD and CRT display models were also evaluated with regard to spectral accuracy and by testing alternate models with less restrictive assumptions. Details of these can be found in an upcoming paper.[13]

A common problem with most AMLCD displays is one of limited viewing-angle. In order to quantify the level of color shifts introduced by off-axis viewing for the prototype LCD display used in this paper, an additional set of measurements was made for the 64 test patches along a viewing-angle of approximately 30 degrees with respect to the normal to the display. Color differences between the measurements for 0-degree and 30-degree angles were computed in absolute (using the white measurement for 0-degrees as the white for conversion of both sets of measurements into CIELAB) and in relative (using measured white-point for each case as the white for conversion to CIELAB) CIELAB space. The mean and maximum color differences over the 64 test patches in $\triangle E_{ab}^*$ and $\triangle E_{94}^*$ units are given in Table 3. For both cases (absolute CIELAB and relative CIELAB), the color differences are quite large and much larger than the color-calibration errors for on-axis viewing. The large

Table 3: Color shifts over test patches between 0 and 30-degree viewing for the LCD display.

	Color Shifts			
	$\triangle E_{ab}^*$ units		$\triangle E_{94}^*$ units	
	Mean	Max.	Mean	Max
Absolute CIELAB	7.94	15.03	4.53	9.24
Relative CIELAB	5.48	11.37	2.86	8.32

magnitude of the differences indicates that the LCD display should only be used for a limited viewing-angle if accurate color is desired. The predominant effect seen in off-axis viewing is a reduction in contrast and saturation, this effect is also obvious from a 3-D visualization of the color shifts.[13] .

5. COMPARISON OF LCD AND CRT DISPLAYS

The AMLCD technology has several advantages over conventional CRT technology. LCD displays have smaller size and are less heavy and bulky than the CRTs, which is the driving force for their increasing use in portable and desktop devices. From an image-quality standpoint, the predominant and most clearly visible advantage is the higher spatial-resolution of the LCD devices, which translates into sharper images.

From the preceding sections, it is clear that LCDs and CRTs are similar in several respects from the perspective of color calibration. Identical models based on channel-independence and channel-chromaticity-constancy can be used for the calibration of either type of display and the run-time mapping of images to display color-coordinates can also be performed using the inverse-model of Fig. 2 in either case. For the CRT, these models provide extremely good accuracy, whereas for LCD displays, the accuracy is good enough for most applications. For the CRT, the use of parametric "gamma-offset" models for the individual channel TRCs can further simplify the characterization process and potentially reduce the number of measurements required. The S-shaped TRCs for LCD displays are not modeled well by the parametric "gamma-offset" models and therefore additional measurements may be required for the characterization of these devices.

CRTs are almost Lambertian[17] radiators within typical viewing-angles[29,30] and can therefore be viewed over a wide range of viewing-angles without loss of contrast or undesirable variations in hue. While many improvements have been made in increasing AMLCD viewing-angles, the problem has not been completely eliminated and the useful viewing-angle range of most LCD displays is limited in comparison to CRTs. The limited viewing-angle of LCD displays is often a limitation when precisely color-corrected images are to be displayed before an audience of more than one or two persons.

For the displays used in the experiment, the luminance of white on the LCD display is about 4.7 times the luminance of white on the CRT monitor. This difference is typical for most LCD and CRT displays.[10] For the measurements made in a completely dark room with with almost no additive flare, the luminance of black on the LCD display was about 58 times the luminance of black on the CRT and the dynamic range (ratio of white to black luminances) is around 357 : 1 for the LCD display and 4351 : 1 for the CRT. On the face of it, the CRT appears to have a larger dynamic range, however, in practice the exact converse is true because a large region of the CRTs dynamic range is lost to additive flare under typical viewing conditions. In the presence of typical viewing flare, the ratio black to white luminance for the CRT falls to 16 : 1 whereas the corresponding ratio for the LCD remains significantly higher at 209 : 1. This reversal is owing to the fact that the typical viewing flare has a much higher luminance than the CRT black in a dark room but is quite negligible as compared to the light leakage through the LCD cells already present in the LCD black. The higher white luminance for the LCD displays gives them a higher effective dynamic range than typical CRTs, which is clearly apparent in practice.

Fig. 5 shows the location of the channel chromaticities (the end points of the respective triangles) for the CRT and the LCD display in relation to the spectrum locus on the CIE xy chromaticity diagram.[15–17] Note that the red channel chromaticity for the CRT and the LCD display are fairly close to each other on the chromaticity diagram, but the blue and green channel chromaticities are different from each other. Also plotted on the same diagram are the chromaticities for the white-point for the CRT (labeled as letter C on the plot),

the LCD display (L) and the CIE D50 and D65 daylight illuminants. Note that the LCD display white-point is somewhere between the D65 and D50 white-points, while the CRT white-point is close to D65 in chromaticity, which agrees with the selected 6500 K color temperature for the CRT. The differences in white-point and in the channel chromaticities imply that the the 3×3 color calibration matrices for the LCD and the CRT display in the model of Fig. 2 are different. This implies that transformation of an image in CRT RGB coordinates to LCD display RGB coordinates requires full color-correction and cannot be achieved by using one-dimensional corrections for each of the channels. While only one LCD display was considered in the experiment of this paper, this implication is probably true in general because there are bound to be variations in LCD display channel chromaticities due to manufacturing tolerances in the fabrication of the LCD filters and back-lights.
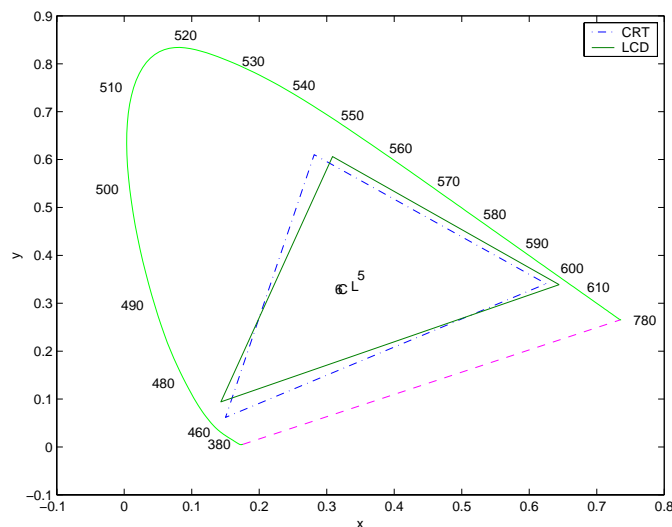

Figure 5. Channel Chromaticities for the LCD and CRT displays in relation to the spectrum locus. Also shown are the white-points C (for CRT), L (for LCD), 6 (CIE D65), and 5 (CIE D50).

The triangle formed by the three channel chromaticity-coordinates for each display in Fig. 5 represents the achievable gamut for the display in chromaticity space. The two-dimensional representation is however rather limited and comparisons of the 3-D gamut in CIELAB coordinates using visualization tools[31] provide a much more complete and useful picture. Since the perception of color is significantly influenced by the viewing conditions,[32] three different gamut comparisons were performed, corresponding to different assumptions for the viewing conditions: 1) comparisons of ideal flare-less "relative" gamuts, where each monitors own white-point was used as the nominal white-point[17] in the conversion from CIEXYZ to CIELAB, 2) comparison of "relative" gamuts with typical flare, and 3) comparison of "absolute" gamuts, where flare is included and the CIEXYZ values for the LCD display white (having the higher luminance) were used in the CIEXYZ to CIELAB conversion for both the measurements from the LCD and the CRT. The first case represents the ideal achievable gamuts assuming that the displays are viewed individually in a dark room and that the photopic response of the eye extends till the black point of the CRT (which does not really hold). The second case corresponds to the more typical situation when the two displays are viewed individually at different times in typical viewing environments. The third case is representative of the scenario when the two displays are viewed side-by-side at the same time (the assumption here is that when the viewer sees the two displays side by side, he/she adapts to the brighter white). For each of the three cases, the 3-D gamuts were computed in CIELAB space and visualized simultaneously with the larger gamut shown as a wire mesh and the smaller gamut as a solid. Figs. 6-8 show perspective views of the gamuts for these different cases, where each figure includes a top-view looking down on the gamuts from the L^* axis and a side-view, whose perspective position was chosen to highlight the gamut differences.

For the flare-less idealized gamuts of Fig. 6, the CRT gamut (wire-frame) and the LCD gamut (solid) are

fairly close in most color regions, except in the blue and magenta regions of color space where the CRT gamut extends further outwards covering a larger volume. The CRT gamut also extends further outward than the LCD gamut in the dark regions close to black. In the presence of typical viewing flare, however, the CRT not only loses its advantage over the LCD but also ends up with significantly smaller gamut in the dark regions. This can be seen from the gamut comparisons of Fig. 7, where the LCD gamut (wire-frame) is significantly larger than the CRT gamut (solid) particularly in the dark color regions around black. The dramatic increase in lightness (L^*) value for the CRT black between Figs. 6 and 7 is indicative of the significant reduction in dynamic range caused by flare, which was mentioned earlier. The significantly larger gamut in the dark color regions provides the LCD displays a significant advantage over CRTs when displaying images with large dynamic range and shadow-detail. Fig. 8 presents a comparison of the LCD (wire-frame) and CRT (solid) gamuts in "absolute" CIELAB (Case 3 above). The "absolute" CRT gamut is almost entirely contained inside the LCD gamut and quite small in comparison. This is primarily due to the much higher luminances of the LCD display. These gamut comparisons also illustrate why the CRT appears quite satisfactory when viewed by itself independently of the LCD display (gamut comparisons of Fig. 7), but seems to be quite "washed out" when viewed side-by-side with the LCD display (gamut comparisons of Fig. 8).

6. CONCLUSIONS

Using a simple offset, matrix, and tone-response correction for the conversion of tristimulus values into display RGB, it is possible to calibrate AMLCD color displays can be color-calibrated with good accuracy (average color error of approx. $1\triangle E_{94}^*$). The raw TRCs for LCDs are S-shaped and are not accurately represented by the "gamma+offset" parametric model commonly used for CRTs. Display calibration techniques that are based on these parametric models should not be directly applied to LCD display color calibration.

The difference between the uncorrected TRCs for AMLCDs and CRTs implies that images designed for CRTs will not have the proper tone-response on these displays, unless appropriate tone-response corrections are used in hardware/software. The LCD display channel-chromaticity coordinates are determined by the back-light and color filter spectral characteristics, and may not correspond to the chromaticity coordinates for commonly employed CRT phosphors. Therefore, a simple per-channel one-dimensional correction cannot be used to universally map CRT RGB to LCD RGB.

The prototype display studied in this paper showed a strong variation in color with change in viewing-angle. This viewing-angle dependence limits the utility of the display in accurate color demonstrations where the display is to be simultaneously viewed by multiple observers. While significant viewing-angle improvements have been made in commercial displays,[10] further improvements are still needed to match CRT viewing-angles.

Typical AMLCD displays possess a significantly larger gamut than typical CRT displays, with the AMLCD gamut extending significantly beyond CRT gamut in the dark color regions. The differences in gamut arise primarily due to the higher luminance of LCDs and provide AMLCD displays a significant advantage over CRTs in the reproduction of images with high dynamic range and shadow detail.

REFERENCES

1. J. A. Castellano, "Trends in the global CRT market," in *SID Intl. Symp. Digest of Tech. Papers*,[33] pp. 356–359.
2. K. I. Werner, "The flat panel's future," *IEEE Spectrum* **30**, pp. 18–26, Nov. 1993.
3. S. L. Wright, R. W. Nywening, S. E. Millman, J. Larimer, J. Gille, and J. Luszcz, "Image quality issues for hight resolutions TFTLCDs," in *Proc. IS&T/SID Seventh Color Imaging Conference: Color Science, Systems and Applications*, pp. 100–105, (Scottsdale, AZ), 16-19 Nov. 1999.
4. W. B. Cowan, "An inexpensive scheme for calibration of a color monitor in terms of standard CIE coordinates," *Comp. Graphics* **17**, pp. 315–321, Jul. 1983.
5. W. B. Cowan and N. Rowell, "On the gun independency and phosphor constancy of colour video monitors," *Color Res. Appl.* **11**, pp. S34–S38, Supplement 1986.
6. D. H. Brainard, "Calibration of a computer controlled color monitor," *Color Res. Appl.* **14**, pp. 23–34, Feb. 1989.

7. V. Mani, "Calibration of color monitors," M. S. thesis, North Carolina State University, 1991.

8. R. S. Berns, R. J. Motta, and M. E. Gorzynski, "CRT Colorimetry. Part I: Theory and practice," *Color Res. Appl.* **18**, pp. 299–314, Oct. 1993.

9. R. S. Berns, M. E. Gorzynski, and R. J. Motta, "CRT Colorimetry. Part II: Metrology," *Color Res. Appl.* **18**, pp. 315–325, Oct. 1993.

10. M. D. Fairchild and D. Wyble, "Colorimetric characterization of the apple studio display (flat panel LCD)." Munsell Color Science Laboratory Technical Report, Jul. 1998.

11. C. Y. Tsai, M. J. Shaw, and H. P. D. Shieh, "Color characterization and reproduction of TN-LCDs," in *SID Intl. Symp. Digest of Tech. Papers*,[33] pp. 790–797.

12. G. Sharma, "Color calibration of DPiX AMLCD display." Xerox Corporation, Internal Memo, May 1999.

13. G. Sharma, "LCD displays vs. CRTs: Color-calibration and gamut considerations," *Proc. IEEE* **90**, Feb. 2002. special issue on Flat Panel Display Technologies, to appear.

14. CIE, "Colorimetry." CIE Publication No. 15.2, Central Bureau of the CIE, Vienna, 1986.

15. G. Sharma and H. J. Trussell, "Digital color imaging," *IEEE Trans. Image Proc.* **6**, pp. 901–932, Jul. 1997.

16. G. Sharma, M. J. Vrhel, and H. J. Trussell, "Color imaging for multimedia," *Proc. IEEE* **86**, pp. 1088–1108, Jun. 1998.

17. G. Wyszecki and W. S. Stiles, *Color Science: Concepts and Methods, Quantitative Data and Formulae*, John Wiley & Sons, Inc., New York, second ed., 1982.

18. C. D. Child, "Discharge from hot CaO," *Phys. Rev.* **32**, pp. 492–511, May 1911.

19. I. Langmuir, "The effect of space charge and residual gases on thermionic current in high vacuum," *Phys. Rev., Second Series* **2**, pp. 450–486, Dec. 1913.

20. B. M. Oliver, "Tone rendition in television," *Proc. IRE* **38**, pp. 1288–1300, 1950.

21. W. N. Sproson, *Colour science in television and display systems*, Adam Hilger Ltd, Bristol, 1983.

22. C. A. Poynton, "Gamma correction and tone reproduction in scanned photographic images," *SMPTE Journal* , pp. 377–385, Jun. 1994.

23. M. A. Karim, ed., *Electro-Optical Displays*, Marcel Dekker, New York, NY, 1992.

24. R. Martin, J. Batey, T. Fiske, M. Nguyen, E. Rabner, D. Siemens, H. Steemers, S. Stuber, M. Thompson, W. Turner, M. Tilton, L. D. Silverstein, and M. Potts, "Design of high-resolution AMLCDs with greater than 2000 gate lines," in *SID Intl. Symp. Digest of Tech. Papers*, pp. 7–10, May 1997.

25. CIE, "Industrial color difference evaluation." CIE Publication No. 116-1995, Central Bureau of the CIE, Vienna, 1995.

26. R. J. Motta, "Visual characterization of color CRTs," in *Proc. SPIE: Device-independent color imaging and imaging systems integration*, R. J. Motta and H. A. Berberian, eds., **1909**, pp. 212–221, Feb. 1993.

27. N. Katoh and T. Deguchi, "Reconsideration of the CRT monitor characteristics," in *Proc. IS&T/SID Fifth Color Imaging Conference: Color Science, Systems and Applications*, pp. 33–40, (Scottsdale, AZ), 17-20 Nov. 1997.

28. T. Deguchi, N. Katoh, and R. S. Berns, "Colorimetric characterization of CRT monitors," in *SID Intl. Symp. Digest of Tech. Papers*,[33] pp. 786–789.

29. J. Kalmer, *Luminescent Screens: Photometry and Colorimetry*, Iliffe, London, 1969.

30. Kinameri, "Photometric error due to light emitting properties of color TV picture tubes," *J. Illum. Eng. Inst. Japan* **67**, pp. 74–79, 1983.

31. R. Rolleston, "Visualization of colorimetric calibration," in *Proc. SPIE: Color hard copy and graphic arts II*, J. Bares, ed., **1912**, pp. 299–309, Feb. 1993.

32. M. D. Fairchild, *Color Appearance Models*, Addison-Wesley, Reading, MA, 1998.

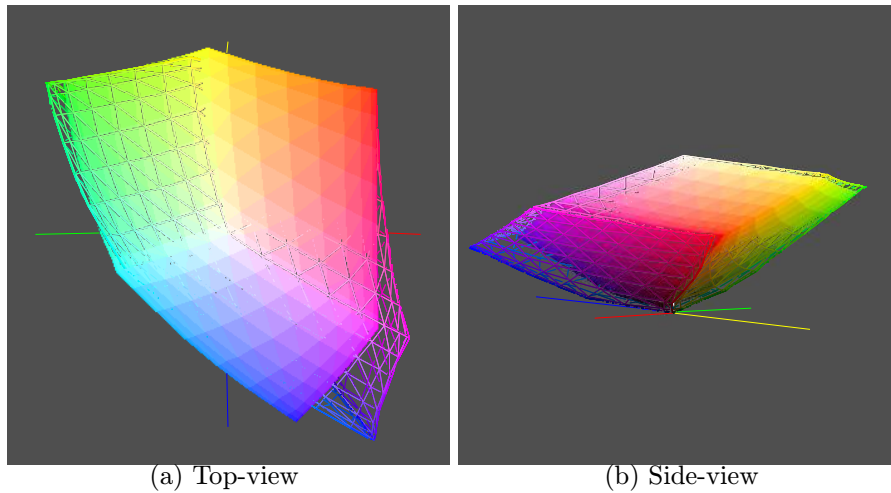33. *SID Intl. Symp. Digest of Tech. Papers*, May 1999.

(a) Top-view   (b) Side-view

Figure 6: Flare-less relative-CIELAB gamuts: LCD (solid), CRT (wire-frame).

(a) Top-view   (b) Side-view
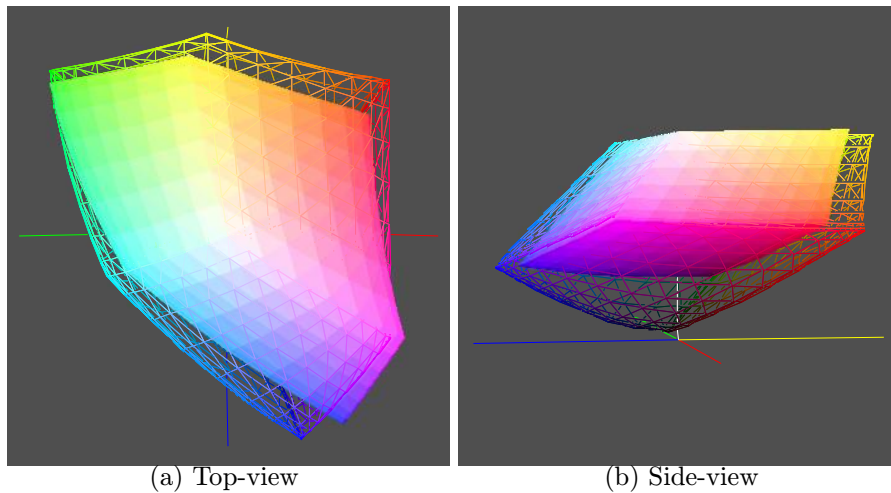
Figure 7: Relative-CIELAB gamuts under normal viewing flare: LCD (wire-frame), CRT (solid).
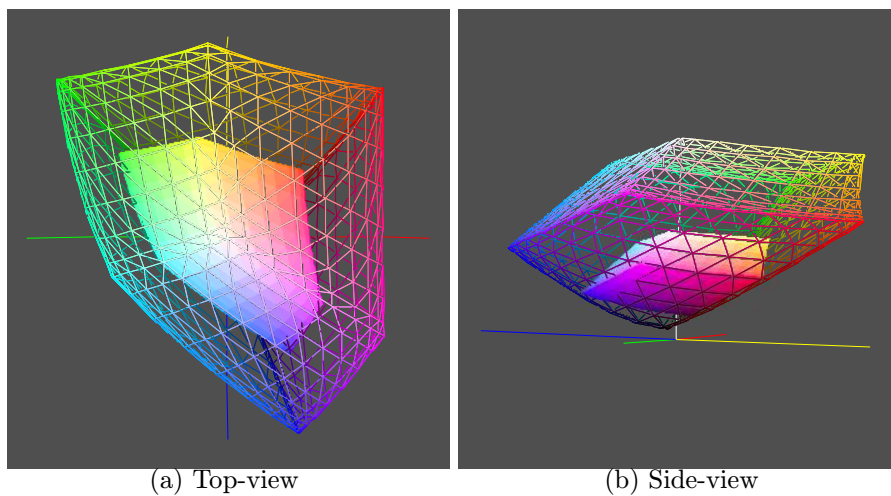

(a) Top-view   (b) Side-view

Figure 8: "Absolute" CIELAB gamuts: LCD (wire-frame), CRT (solid).

Downloaded from SPIE Digital Library on 16 Mar 2011 to 128.151.164.111. Terms of Use: http://spiedl.org/terms